Dalton Transactions

Dynamic Article Links ▶

PAPER

Hydrothermal synthesis, crystal structures, and luminescent properties of a series of new lanthanide oxalatophosphonates with a layer architecture†

Yan-Yu Zhu,[a] Zhen-Gang Sun,*[a] Fei Tong,[a] Zhong-Min Liu,[b] Cui-Ying Huang,[a] Wei-Nan Wang,[a] Cheng-Qi Jiao,[a] Cheng-Lin Wang,[a] Chao Li[a] and Kai Chen[a]

Eleven new lanthanide oxalatophosphonate hybrids with a 2D layered structures, namely, $[Ln(H_3L)(C_2O_4)] \cdot 2H_2O$ (Ln = La–Dy, Er and Y, $H_4L = C_6H_5CH_2N(CH_2PO_3H_2)_2$), have been synthesized under hydrothermal conditions and structurally characterized by X-ray single-crystal diffraction, X-ray powder diffraction, infrared spectroscopy, elemental analysis and thermogravimetric analysis. Compounds **1–11** are isomorphous and they exhibit a 2D framework structure. Two $\{LnO_8\}$ polyhedra and four $\{CPO_3\}$ tetrahedra are interconnected into a unit *via* corner-sharing, and the so-built units are bridged by the oxalate anions into a layer. The result of connections in this manner is the formation of a 24-atom window. The thermal stabilities and guest desorption–sorption properties of compounds **1–11** have been investigated. The luminescent properties of compounds **5**, **6**, **8** and **9** have also been studied.

Introduction

In recent years, much attention has been drawn to the construction of metal phosphonates due to their potential applications in catalysts, ion exchangers, sorbents, meso-/microporous materials, or intercalation chemistry.[1] The rational design and assembly of metal phosphonates with well-regulated network structures has received remarkable attention in order to develop new functional materials with potential applications. So far, a great number of metal phosphonates with intriguing structures have been successfully prepared through designing and synthesizing phosphonic acids and the careful selection of metal ions.[2] Lanthanide ions, as functional metal-center ions with optical and magnetic properties, show a wide range of potential technological applications, such as optoelectronic devices and fluoroimmunoassays.[3] Phosphonic acid has been exploited as one of the most attractive ligands for building lanthanide-containing materials because of its versatile coordination modes, as well as the good thermal and chemical stabilities of the Ln–O–P bonds that phosphonate ligands make with lanthanide ions.

Therefore, lanthanide phosphonates can exhibit intense luminescence that has found applications in fluorescent probes and electroluminescent devices.[4] However, lanthanide phosphonates normally have low solubility and poor crystallinity, hence, the further exploitation of such materials is still limited. To improve the solubility and crystallinity of lanthanide phosphonates, additional function groups such as crown ether, carboxylate, hydroxyl and amine groups have been attached to the phosphonate ligand. Some substantial progress has been made by Clearfield, Ferey, Lukes, Lin and Bligh *et al.*[5] It was found that introducing a suitable ancillary ligand such as carboxylic acid into the lanthanide phosphonate system can also improve the solubility and crystallinity of lanthanide phosphonates. In recent years, a series of lanthanide phosphonates with carboxylic acid as a second ligand have been reported by Mao *et al.*[6] Among these auxiliary ligands, oxalate was found to be an efficient assistant because of its versatile coordination modes, as well as the high and variable coordination number of lanthanide ions. More importantly, due to the π-conjugated character, the divalent oxalate anion is an effective bridge for charge and energy transfer between metal centers that it links, making it a good chromophore and therefore useful as a lanthanide luminescence sensitizer. Additionally, the coordination of two types of ligands with the lanthanide ion may reduce or eliminate water molecules from the coordination sphere of the lanthanide(III) ion, hence increasing the luminescent intensity and lifetime of the materials.[4a] By using phosphonic acids as the ligands and the oxalate moiety, $C_2O_4^{2-}$, as the second metal linker, a series of novel lanthanide oxalatophosphonate hybrids with 3D framework structures have been obtained by our group.[7] However, reported lanthanide oxalatephosphonates with definite structures are still rare, and most of the lanthanide oxalatophosphonates show 3D framework structures. As an extension of our previous work, we selected *N*-benzyliminobis(methylenephosphonic acid), $C_6H_5CH_2N(CH_2PO_3H_2)_2$ (H_4L) as the phosphonate ligand and

[a]Institute of Chemistry for Functionalized Material, School of Chemistry and Chemical Engineering, Liaoning Normal University, Dalian, 116029, P. R. China. E-mail: szg188@163.com; Fax: +86 411 82156989
[b]Dalian Institute of Chemical Physics, Chinese Academy of Sciences, Dalian, 116023, P. R. China

† Electronic supplementary information (ESI) available: XRD patterns, IR spectra for compounds **1–11**, XRD patterns of the final products in the thermal decomposition for compound **6**, and tables listing selected bond lengths and bond angles for compounds **1–7** presented in this paper. CCDC reference numbers 705728–705734. For ESI and crystallographic data in CIF or other electronic format see DOI: 10.1039/c0dt01781g

oxalate as the second metal linker. Our research efforts afforded eleven new lanthanide oxalatophosphonate hybrids with 2D layered structures, namely, [Ln(H$_3$L)(C$_2$O$_4$)]·2H$_2$O (Ln = La–Dy, Er and Y). Herein we report their syntheses, crystal structures, thermal stabilities, guest desorption–sorption and luminescence properties.

Experimental

Materials and measurements

The *N*-benzyliminobis(methylenephosphonic acid), C$_6$H$_5$CH$_2$N-(CH$_2$PO$_3$H$_2$)$_2$ (H$_4$L), was prepared by a Mannich type reaction according to the procedures previously described.[8] The lanthanide(III) chlorides were prepared by dissolving corresponding lanthanide oxides (General Research Institute for Nonferrous Metals, 99.99%) in hydrochloric acid followed by recrystallization and drying. All other chemicals were used as received without further purification. C, H and N were determined by using a PE-2400 elemental analyzer. La, Ce, Pr, Nd, Sm, Eu, Gd, Tb, Dy, Er, Y and P were determined by using an inductively coupled plasma (ICP) atomic absorption spectrometer. IR spectra were recorded on a Bruker AXS TENSOR–27 FT–IR spectrometer with KBr pellets in the range 4000–400 cm^{-1}. The X-ray powder diffraction data was collected on a Bruker AXS D8 Advance diffractometer using Cu-Kα radiation (λ = 1.5418 Å) in the 2θ range of 5–50°/60° with a step size of 0.02° and a scanning rate of 3° min^{-1}. The luminescence spectra were reported on a HITACHI F–4600 spectrofluorimeter (solid). TG analyses were performed on a Perkin–Elmer Pyris Diamond TG–DTA thermal analyses system in static air with a heating rate of 10 K min^{-1} from 50 °C to 1100 °C.

Synthesis

Synthesis of [La((HO$_3$PCH$_2$)$_2$NHCH$_2$C$_6$H$_5$)(C$_2$O$_4$)]·2H$_2$O (1).
A mixture of LaCl$_3$·6H$_2$O (0.18 g, 0.50 mmol), H$_4$L (0.30 g, 1.00 mmol), H$_2$C$_2$O$_4$·2H$_2$O (0.25 g, 2.00 mmol), and NaOH (0.08 g, 2.00 mmol) was dissolved in 10 mL distilled water. The resulting solution was stirred for about 1 h at room temperature, sealed in a 20 mL Teflon-lined stainless steel autoclave, and heated at 100 °C for 4 days under autogenous pressure. After the mixture was cooled slowly to room temperature, the colorless plate crystals were obtained in *ca*. 86.8% yield based on La. Anal. calcd (%) for C$_{11}$H$_{18}$NO$_{12}$P$_2$La (557.11): C 23.71, H 3.23, N 2.51, P 11.12, La 24.93. Found: C 23.76, H 3.40, N 2.58, P 11.05, La 24.86.

Synthesis of [Ce((HO$_3$PCH$_2$)$_2$NHCH$_2$C$_6$H$_5$)(C$_2$O$_4$)]·2H$_2$O (2).
The procedure was the same as that for **1** except that LaCl$_3$·6H$_2$O was replaced by CeCl$_3$·7H$_2$O (0.19 g, 0.50 mmol). Colorless plate crystals of **2** were obtained and washed with water. Yield: 64.3% based on Ce. Anal. calcd (%) for C$_{11}$H$_{18}$NO$_{12}$P$_2$Ce (558.32): C 23.66, H 3.22, N 2.51, P 11.09, Ce 25.10. Found: C 23.62, H 3.15, N 2.43, P 11.01, Ce 25.18.

Synthesis of [Pr((HO$_3$PCH$_2$)$_2$NHCH$_2$C$_6$H$_5$)(C$_2$O$_4$)]·2H$_2$O (3).
The procedure was the same as that for **1** except that LaCl$_3$·6H$_2$O was replaced by PrCl$_3$·6H$_2$O (0.18 g, 0.50 mmol). Green plate crystals of **3** were obtained and washed with water. Yield: 89.5% based on Pr. Anal. calcd (%) for C$_{11}$H$_{18}$NO$_{12}$P$_2$Pr (559.11): C 23.63, H 3.22, N 2.51, P 11.08, Pr 25.20. Found: C 23.54, H 3.15, N 2.46, P 11.13, Pr 25.28.

Synthesis of [Nd((HO$_3$PCH$_2$)$_2$NHCH$_2$C$_6$H$_5$)(C$_2$O$_4$)]·2H$_2$O (4).
The procedure was the same as that for **1** except that LaCl$_3$·6H$_2$O was replaced by NdCl$_3$·6H$_2$O (0.18 g, 0.50 mmol). Purple plate crystals of **4** were obtained and washed with water. Yield: 60.7% based on Nd. Anal. calcd (%) for C$_{11}$H$_{18}$NO$_{12}$P$_2$Nd (562.44): C 23.49, H 3.20, N 2.49, P 11.01, Nd 25.65. Found: C 23.42, H 3.14, N 2.45, P 11.08, Nd 25.58.

Synthesis of [Sm((HO$_3$PCH$_2$)$_2$NHCH$_2$C$_6$H$_5$)(C$_2$O$_4$)]·2H$_2$O (5).
The procedure was the same as that for **1** except that LaCl$_3$·6H$_2$O was replaced by SmCl$_3$·6H$_2$O (0.19 g, 0.50 mmol). Pale yellow plate crystals of **5** were obtained and washed with water. Yield: 77.5% based on Sm. Anal. calcd (%) for C$_{11}$H$_{18}$NO$_{12}$P$_2$Sm (568.55): C 23.24, H 3.17, N 2.46, P 10.89, Sm 26.45. Found: C 23.16, H 3.09, N 2.51, P 10.81, Sm 26.53.

Synthesis of [Eu((HO$_3$PCH$_2$)$_2$NHCH$_2$C$_6$H$_5$)(C$_2$O$_4$)]·2H$_2$O (6).
The procedure was the same as that for **1** except that LaCl$_3$·6H$_2$O was replaced by EuCl$_3$·6H$_2$O (0.19 g, 0.50 mmol). Colorless plate crystals of **6** were obtained and washed with water. Yield: 87.3% based on Eu. Anal. calcd (%) for C$_{11}$H$_{18}$NO$_{12}$P$_2$Eu (570.16): C 23.17, H 3.16, N 2.46, P 10.86, Eu 26.65. Found: C 23.11, H 3.09, N 2.52, P 10.90, Eu 26.72.

Synthesis of [Gd((HO$_3$PCH$_2$)$_2$NHCH$_2$C$_6$H$_5$)(C$_2$O$_4$)]·2H$_2$O (7).
The procedure was the same as that for **1** except that LaCl$_3$·6H$_2$O was replaced by GdCl$_3$·6H$_2$O (0.19 g, 0.50 mmol). Colorless plate crystals of **7** were obtained and washed with water. Yield: 76.5% based on Gd. Anal. calcd (%) for C$_{11}$H$_{18}$NO$_{12}$P$_2$Gd (575.45): C 22.96, H 3.13, N 2.43, P 10.76, Gd 27.33. Found: C 22.88, H 3.18, N 2.39, P 10.68, Gd 27.26.

Synthesis of [Tb((HO$_3$PCH$_2$)$_2$NHCH$_2$C$_6$H$_5$)(C$_2$O$_4$)]·2H$_2$O (8).
The procedure was the same as that for **1** except that LaCl$_3$·6H$_2$O was replaced by TbCl$_3$·6H$_2$O (0.19 g, 0.50 mmol). Colorless plate crystals of **8** were obtained and washed with water. Yield: 70.6% based on Tb. Anal. calcd (%) for C$_{11}$H$_{18}$NO$_{12}$P$_2$Tb (577.12): C 22.89, H 3.12, N 2.43, P 10.73, Tb 27.54. Found: C 22.82, H 3.05, N 2.48, P 10.68, Tb 27.61.

Synthesis of [Dy((HO$_3$PCH$_2$)$_2$NHCH$_2$C$_6$H$_5$)(C$_2$O$_4$)]·2H$_2$O (9).
The procedure was the same as that for **1** except that LaCl$_3$·6H$_2$O was replaced by DyCl$_3$·6H$_2$O (0.19 g, 0.50 mmol). Colorless plate crystals of **9** were obtained and washed with water. Yield: 83.4% based on Dy. Anal. calcd (%) for C$_{11}$H$_{18}$NO$_{12}$P$_2$Dy (580.70): C 22.75, H 3.10, N 2.41, P 10.67, Dy 27.98. Found: C 22.68, H 3.15, N 2.35, P 10.59, Dy 28.06.

Synthesis of [Er((HO$_3$PCH$_2$)$_2$NHCH$_2$C$_6$H$_5$)(C$_2$O$_4$)]·2H$_2$O (10).
The procedure was the same as that for **1** except that LaCl$_3$·6H$_2$O was replaced by ErCl$_3$·6H$_2$O (0.19 g, 0.50 mmol). Pink plate crystals of **10** were obtained and washed with water. Yield: 86.6% based on Er. Anal. calcd (%) for C$_{11}$H$_{18}$NO$_{12}$P$_2$Er (585.46): C 22.57, H 3.07, N 2.39, P 10.58, Er 28.57. Found: C 22.51, H 3.12, N 2.32, P 10.51, Er 28.65.

Synthesis of [Y((HO$_3$PCH$_2$)$_2$NHCH$_2$C$_6$H$_5$)(C$_2$O$_4$)]·2H$_2$O (11).
The procedure was the same as that for **1** except that LaCl$_3$·6H$_2$O was replaced by YCl$_3$·6H$_2$O (0.15 g, 0.50 mmol). Colorless plate crystals of **11** were obtained and washed with water. Yield: 87.6% based on Y. Anal. calcd (%) for C$_{11}$H$_{18}$NO$_{12}$P$_2$Y (507.11): C 26.05,

H 3.55, N 2.76, P 12.21, Y 17.53. Found: C 26.12, H 3.48, N 2.71, P 12.28, Y 17.45.

X-Ray crystallographic analysis

Data collections for compounds **1–7** were performed on the Bruker AXS Smart APEX II CCD X–diffractometer equipped with graphite monochromated Mo-Kα radiation ($\lambda = 0.71073$ Å) at 293 ± 2 K. An empirical absorption correction was applied using the SADABS program. The structures were solved by direct methods and refined by full matrix least-squares on F^2 by using the programs SHELXS-97.[9] All non-hydrogen atoms were refined anisotropically. All hydrogen atoms were placed in geometrically idealized positions and constrained to ride on their parent atoms. The final difference Fourier maps for compound **1** showed residual peaks of 2.221 e Å^{-3} (0.94 Å from La1 atom) and holes of -1.186 e Å^{-3} (0.95 Å from La1 atom). The final difference Fourier maps for compound **7** showed residual peaks of 2.553 e Å^{-3} (1.00 Å from Gd1 atom) and holes of -0.91 e Å^{-3} (1.04 Å from O2 atom). The relatively higher residuals are due to the absorption correction problems with the heavy Ln(III) ions. Details of crystallographic data of compounds **1–7** are summarized in Table 1. Selected bond lengths and angles are given in Table S1 and Table S2 (ESI†).

Results and discussion

Synthesis

Compounds **1–11** were prepared under hydrothermal conditions by reaction of lanthanide(III) chlorides, oxalate and the diphosphonate ligand (H$_4$L). NaOH was added into the reaction system directly in the form of a solid, which was employed as the inorganic base to adjust the pH of the reaction mixture. It was found that pure phases of compounds **1–11** were observed in the reactions containing Ln^{3+}, H$_4$L, H$_2$C$_2$O$_4$·2H$_2$O and NaOH in the molar ratio 1 : 2 : 4 : 4. The initial and final pH values of the resultant solution are about 1 and 2, respectively. In addition, the reaction temperature was very important for the formation of suitable single-crystals for X-ray diffraction. The compounds **1–11** were obtained after heating at 100 °C for 4 days under hydrothermal conditions. However, the best crystallinity of the reaction product was observed in compounds **1–7**. Despite all our efforts to grow big single-crystals of compounds **8–11**, we were not successful in obtaining a good sample for X-ray diffraction study. The powder XRD patterns of compounds **1–11** and the simulated XRD patterns are shown in the Supplementary Information (Fig. S1†). The measured XRD patterns of compounds **1–11** are all essentially in agreement with those simulated from X-ray single-crystal data, which indicate these eleven compounds are isomorphous and phase pure. The results of this study provide further evidence that the molar ratio of starting materials and the pH value play an important role in the growth of high quality single crystals.

Description of the crystal structures

Compounds **1–11** are isomorphous and feature a two-dimensional (2D) layered structure, hence only the structure of **1** will be discussed in detail as a representative example. The ORTEP diagram for compound **1** is shown in Fig. 1. Crystallographic data and structural refinements for compounds **1–7** are summarized in Table 1.

Table 1 Crystal data and structure refinements for compounds **1–7**

	1	2	3	4	5	6	7
Formula	C$_{11}$H$_{18}$NO$_{12}$P$_2$La	C$_{11}$H$_{18}$NO$_{12}$P$_2$Ce	C$_{11}$H$_{18}$NO$_{12}$P$_2$Pr	C$_{11}$H$_{18}$NO$_{12}$P$_2$Nd	C$_{11}$H$_{18}$NO$_{12}$P$_2$Sm	C$_{11}$H$_{18}$NO$_{12}$P$_2$Eu	C$_{11}$H$_{18}$NO$_{12}$P$_2$Gd
Mr	557.11	558.32	559.11	562.44	568.55	570.16	575.45
Crystal system	Monoclinic	Monoclinic	Monoclinic	Monoclinic	Monoclinic	Monoclinic	Monoclinic
Space group	$C2/c$	$C2/c$	$C2/c$	$C2/c$	$C2/c$	$C2/c$	$C2/c$
a/Å	28.085(9)	28.090(3)	28.101(4)	28.155(5)	28.210(5)	28.298(3)	28.425(17)
b/Å	9.131(3)	9.0958(9)	9.0522(13)	9.0228(14)	8.9618(15)	8.9336(9)	8.924(5)
c/Å	17.632(6)	17.5746(17)	17.536(3)	17.505(3)	17.405(3)	17.3809(18)	17.391(10)
β/°	126.854(3)	126.8630(10)	126.941(2)	126.884(2)	126.717(2)	126.5920(10)	126.617(7)
V/Å^3	3618(2)	3592.6(6)	3565.1(9)	3556.8(10)	3527.2(11)	3527.9(6)	3541(4)
Z, D_c/g cm^{-3}	8, 2.046	8, 2.065	8, 2.083	8, 2.101	8, 2.141	8, 2.147	8, 2.159
μ/mm^{-1}	2.602	2.776	2.977	3.164	3.576	3.802	3.992
$F(000)$	2192	2200	2208	2216	2232	2240	2248
Crystal size/mm	$0.15 \times 0.12 \times 0.08$	$0.18 \times 0.14 \times 0.09$	$0.06 \times 0.04 \times 0.02$	$0.19 \times 0.10 \times 0.02$	$0.22 \times 0.16 \times 0.04$	$0.20 \times 0.17 \times 0.03$	$0.17 \times 0.09 \times 0.06$
Theta range/°	1.81 to 26.49	2.32 to 26.50	1.81 to 26.49	1.81 to 26.50	1.80 to 26.00	2.34 to 26.00	2.34 to 26.00
Limiting indices	$-28 \leq h \leq 35$, $-10 \leq k \leq 11$, $-22 \leq l \leq 22$	$-22 \leq h \leq 35$, $-11 \leq k \leq 11$, $-22 \leq l \leq 17$	$-27 \leq h \leq 35$, $-11 \leq k \leq 10$, $-22 \leq l \leq 22$	$-35 \leq h \leq 35$, $-11 \leq k \leq 10$, $-16 \leq l \leq 21$	$-34 \leq h \leq 34$, $-10 \leq k \leq 11$, $-21 \leq l \leq 18$	$-34 \leq h \leq 34$, $-11 \leq k \leq 7$, $-19 \leq l \leq 21$	$-34 \leq h \leq 34$, $-8 \leq k \leq 11$, $-21 \leq l \leq 18$
Reflections collected/unique	9765/3740	9812/3716	9786/3687	9758/3679	9368/3454	9134/3452	9327/3469
R_{int}	0.0454	0.0313	0.0579	0.0717	0.0741	0.0398	0.0654
Completeness to theta	26.49, 99.7%	26.50, 99.7%	26.49, 99.8%	26.50, 99.8%	26.00, 99.7%	26.00, 99.8%	26.00, 99.7%
GOF on F^2	1.000	1.022	0.996	0.973	0.999	1.001	1.009
R_1, wR_2 [$I > 2\sigma(I)$][a]	0.0412, 0.0943	0.0254, 0.0542	0.0392, 0.0696	0.0439, 0.0785	0.0450, 0.0833	0.0290, 0.0612	0.0445, 0.0923
R_1, wR_2 (all data)[a]	0.0571, 0.1038	0.0341, 0.0576	0.0622, 0.0785	0.0756, 0.0907	0.0740, 0.0955	0.0409, 0.0664	0.0685, 0.1033
Largest diff. peak and hole/e Å^{-3}	2.221 and -1.186	0.589 and -0.505	0.728 and -0.904	0.851 and -0.814	0.788 and -0.950	0.638 and -0.849	2.553 and -0.914

[a] $R_1 = \Sigma \, (\,|F_0| - |F_C|\,) \, / \, \Sigma \, |F_0|$; $wR_2 = [\Sigma \, w \, (\,|F_0| - |F_C|\,)^2 \, / \, \Sigma \, w \, F_0{}^2]^{1/2}$
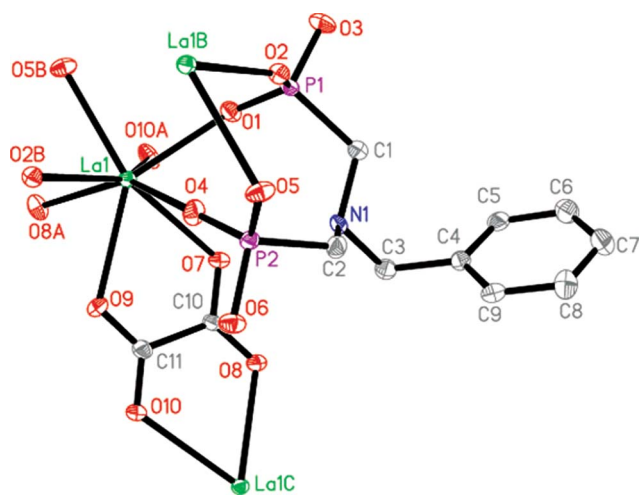
Fig. 1 ORTEP representation of a selected unit of compound **1**. The thermal ellipsoids are drawn at the 50% probability level. All H atoms and solvate water molecules are omitted for clarity. Symmetry code: (A) $-x + 1/2$, $y - 1/2$, $-z + 3/2$; (B) $-x + 1/2$, $-y + 3/2$, $-z + 1$; (C) $-x + 1/2$, $y + 1/2$, $-z + 3/2$.

The asymmetric unit of **1** contains one La(III) ion, one H_3L^- ligand, one oxalate anion and two solvate water molecules. As shown in Fig. 1, La(III) ion is eight-coordinated by four phosphonate oxygen atoms (O1, O4, O2B and O5B) from two H_3L^- ligands and four oxygen atoms (O7, O9, O8A and O10A) from two oxalate anions. Its coordination geometry can be described as a square antiprism,[10] which is different from the coordination geometry of La(III) ion in $[La_2(ox)_2(H_6L)]\cdot2H_2O$.[6c] The bond lengths of La–O are between 2.410(4) and 2.591(4) Å (Table S1, ESI†), and the angles around the La atom are in the range of 63.37(12)–151.35(12)° (Table S2, ESI†), which are comparable to those reported for other lanthanum(III) phosphonates.[6] The oxalate anion is bidentate, and it chelates with two different La(III) ions (La1 and La1C) by using its four carboxylate oxygen atoms (O7, O9, O8 and O10). Such configuration is favorable because of the formation of five-membered chelating rings (La–O–C–C–O). The H_3L^- anion is a tetradentate ligand, chelating bidentately to two La^{3+} ions (La1 and La1B) by using two phosphonate groups (Scheme 1a). Both phosphonate groups of the H_3L^- ligand are singly protonated (O3, O6) based on the requirement of charge balance as well as P–O bond distances. The nitrogen atoms of the amine groups are protonated based on of the requirement of charge balance. Though the protonation

mode of H_3L^- anion in **1** is the same as that in $Ln(H_2L)(H_3L)$,[11] it adopts a different coordination mode. The asymmetric unit of $Ln(H_2L)(H_3L)$ consists of two phosphonate ligands which adopt two different types of coordination modes. The H_3L^- anion acts as a tridentate ligand, one phosphonate group is monodentate whereas the other one is bidentate bridging (Scheme 1b). The H_2L^{2-} anion functions as a tetradentate ligand, being chelated bidentately to two metal centres by using one phosphonate group and also bridging to the third Ln(III) atom (Scheme 1c) via the other phosphonate group.

The overall structure can be described as the stacking of 2D layers along the a-axis. Two $\{LnO_8\}$ polyhedra and four $\{CPO_3\}$ tetrahedra are interconnected into a unit via corner-sharing (Fig. 2a). The so-built units are bridged by the oxalate anions into a layer (Fig. 2b). The interlayer distance is $ca.$ 23.2 Å, and the phenyl groups of the ligands are orientated toward the interlayer space (Fig. 2c). The solvate water molecules are located between two adjacent layers. The result of connections in this manner is the formation of a 24-atom window (Fig. 2d). The window consists of six La, two P, twelve O and four C atoms,
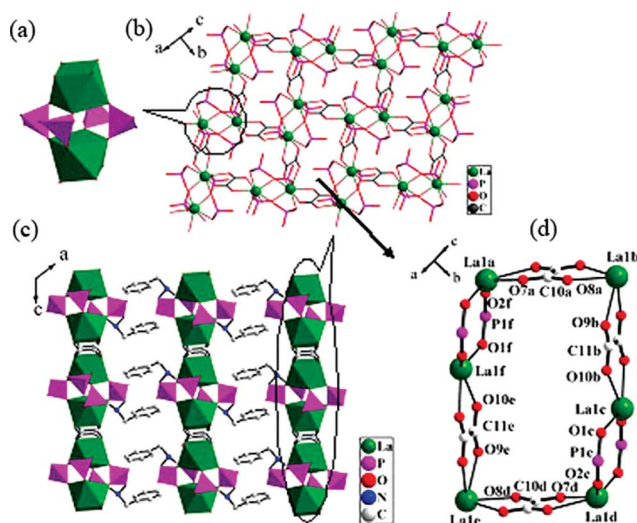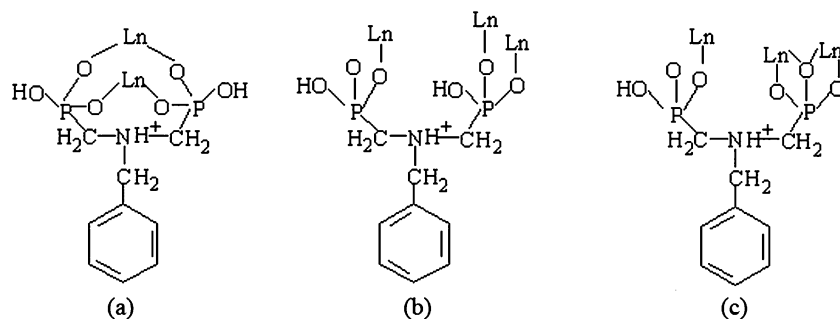

Fig. 2 (a) A polyhedral drawing of the $\{(LaO_8)_2(CPO_3)_4\}$ unit. (b) A 2D layer in compound **1**. (c) The layer structure of compound **1** viewed along b-axis direction. (d) The 24-atom window in compound **1**. Symmetry codes: (a) x, y, $z + 1$; (b) $-x + 1/2$, $y + 1/2$, $-z + 5/2$; (c) x, $y + 1$, $z + 1$; (d) $-x + 1/2$, $-y + 1/2$, $-z + 2$; (e) x, $-y$, $z + 1/2$; (f) $-x + 1/2$, $-y - 1/2$, $-z + 2$.

Scheme 1 Coordination fashions of phosphonate ligands in compound **1** and $[Ln(H_2L)(H_3L)]$.

and the approximate dimension is 11.9 Å (La1a–La1d) × 13.7 Å (La1b–La1e).

IR spectra

The IR spectra of the eleven compounds have many similar features corresponding to the common groups (Fig. S2, ESI†), thus only the spectrum of compound **6** will be discussed. The IR spectrum for compound **6** was recorded in the region 4000–400 cm⁻¹ (Fig. S3, ESI†). Two bands are observed at 3624 and 3523 cm⁻¹, which are due to the O–H stretching vibrations of the water molecules. The band centered at 3421 cm⁻¹ is attributed to the N–H stretching vibrations.[12,13b] The C–H stretching vibrations are observed as sharp, weak bands close to 3000 cm⁻¹. Two pairs of week bands centered at 2858, 2805 and 2403, 2314 cm⁻¹ are likely due to ν(P–OH) and the overtone 2δ(P–O–H), respectively. These bands are characteristic of the hydrogen phosphonate groups.[13] There are two strong bands (1679 cm⁻¹ and 1616 cm⁻¹) and two week bands (1460 cm⁻¹ and 1320 cm⁻¹), which are assigned to the antisymmetrical and symmetrical stretching vibrations of C–O groups when present as COO⁻ moieties.[14] Strong bands between 1200 and 900 cm⁻¹ are due to stretching vibrations of the tetrahedral CPO_3 groups, as expected.[15] Additional weak bands at low energy are found. These bands are probably due to bending vibrations of the tetrahedral CPO_3 groups.

Thermal properties

To identify the stability of the whole frameworks, thermal gravimetric analysis (TGA) and powder X-ray diffraction (PXRD) measurements were performed. The thermal analyses of compounds **1–11** have been performed in the 50–1100 °C temperature range in a static air atmosphere (see Fig. 3). These compounds show similar TGA curves, and compound **6** was used as an example to illustrate the weight losses in detail. The TGA curve of compound **6** reveals three main steps of weight losses. The first step started at 50 °C and was completed at 160 °C, corresponding to the release of two solvate water molecules. The observed weight loss of 6.7% is very close to the calculated value (6.3%). The second step between 275 °C and 500 °C can be attributed to decomposition of the oxalate and phosphonate units. The third step covers a
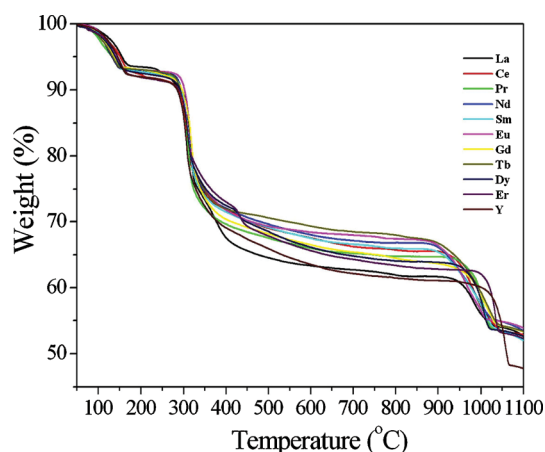
temperature range of 870–1017 °C, which corresponds to the further decomposition of the compound. The final product is the mixture of $Eu(PO_3)_3$ and $EuPO_4$ based on XRD powder studies (Fig. S4, ESI†). The total weight loss of 44.8% is close to the calculated value (44.2%) if the final product is assumed to be mixture of $Eu(PO_3)_3$ and $EuPO_4$ in a molar ratio of 1 : 1. The much larger total weight loss for compound **11** (51.7%) is due to its having a much smaller formula weight than the other compounds. During the thermal decomposition, intermediate compounds may be formed between 500 and 870 °C for compound **6**. In order to identify the intermediate compound, X-ray powder diffraction studies were performed for compound **6** calcined at 700 °C. However, these intermediate compounds were not identified because complicated mixtures were obtained during the thermal decomposition. Considering the thermal stability of these compounds, X-ray powder diffraction studies were performed for the as-synthesized compound **6** and the samples calcined at 180 °C. The powder X-ray diffraction (PXRD) patterns for the dehydrated sample of **6** are different from that of the as-synthesized sample (see Fig. 4), suggesting the occurrence of a certain structural transformation upon evacuation. Interestingly, when this solid was suspended in water, the same PXRD patterns as those of the original crystal were regenerated. Thus, the dehydrated solids of these compounds may be potential reversible adsorbent materials for water molecules.
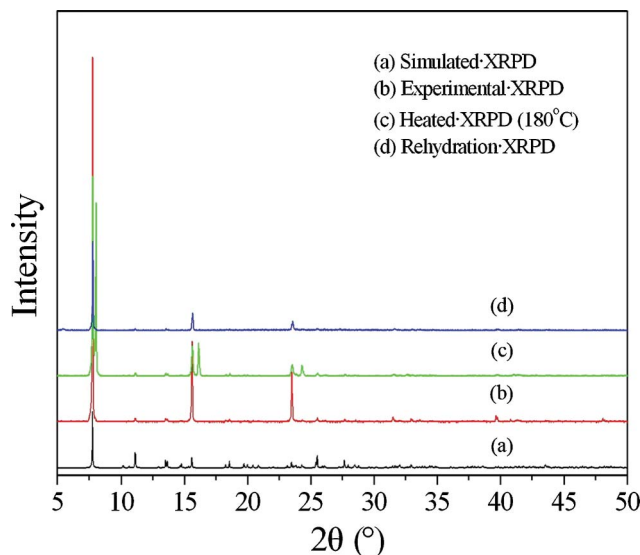

Fig. 4 Experimental, heated (180 °C) and rehydrated X-ray powder diffraction diagram of compound **6** compared to the calculated one.

Luminescent properties

It is well-known that the lanthanides, especially europium and terbium, can absorb ultraviolet radiation efficiently through an allowed electronic transition to convert to the excited state $^5D_4$, and these excited states are deactivated to the multiplet ^7F_J states radiatively *via* emission of visible radiation as luminescence. The luminescent behaviors of the Sm (**5**), Eu (**6**), Tb (**8**) and Dy (**9**) compounds were investigated in the solid state at room temperature. The emission spectrum of compound **5** at the excited wavelength of 404 nm is shown in Fig. 5a. There are three
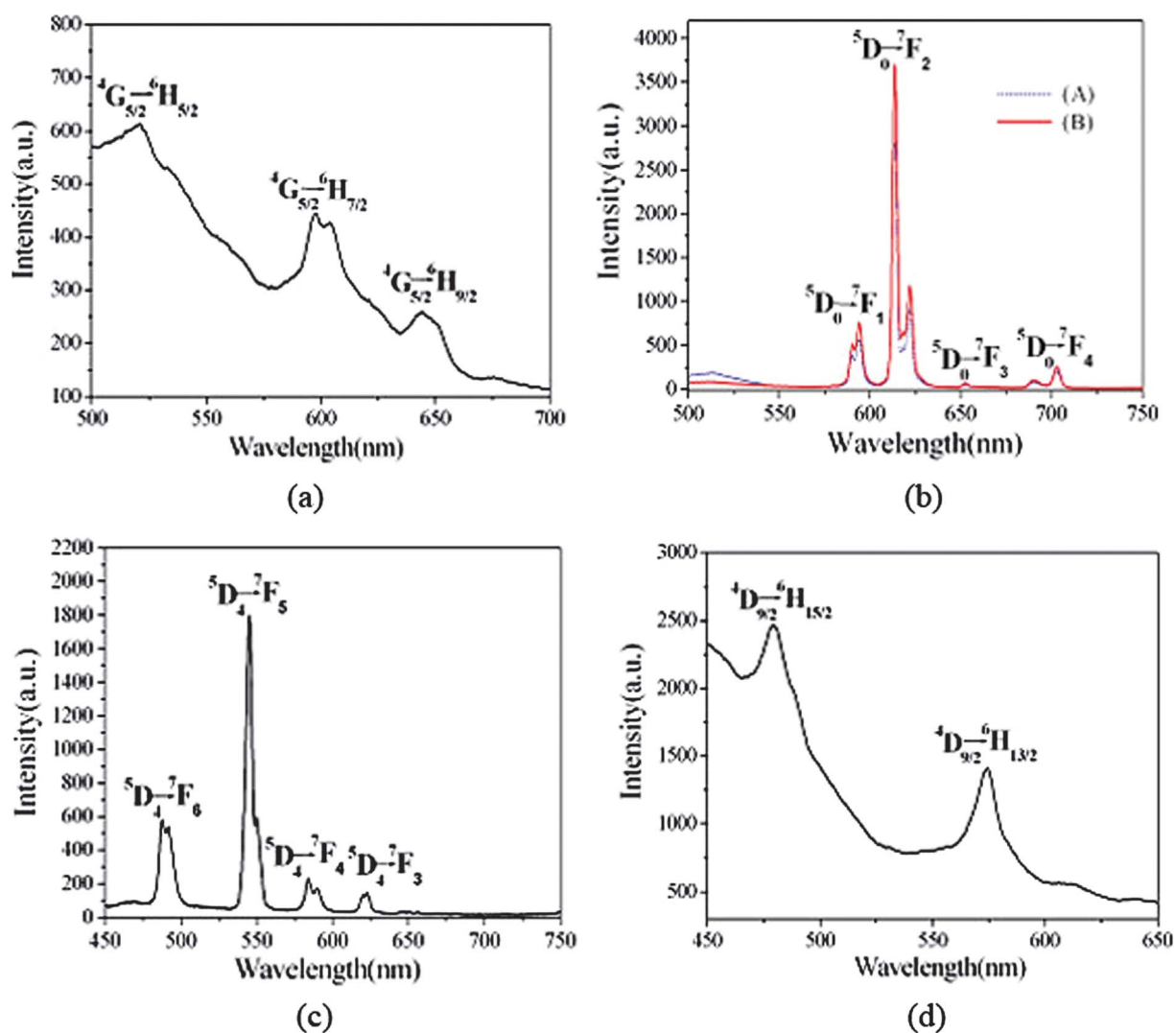

Fig. 3 TGA curves of compounds **1–11**.

Fig. 5 (a) Solid-state emission spectrum of compound **5** at room temperature. (b) Solid-state emission spectra of experimental (A) and dehydrated (B) samples of compound **6** at room temperature. (c) Solid-state emission spectrum of compound **8** at room temperature. (d) Solid-state emission spectrum of compound **9** at room temperature.

characteristic bands, which are attributed to $^4G_{5/2} \rightarrow {}^6H_J$ (J = 5/2, 7/2, 9/2), $^4G_{5/2} \rightarrow {}^6H_{5/2}$ (520 nm), $^4G_{5/2} \rightarrow {}^6H_{7/2}$ (597 nm), and $^4G_{5/2} \rightarrow {}^6H_{9/2}$ (644 nm) transitions.[16] Compound **6** exhibits four sets of characteristic emission bands for the Eu(III) ion in the visible region under excitation at 397 nm (Fig. 5b). These emission bands are 590 and 594 nm (weak, $^5D_0 \rightarrow {}^7F_1$), 614 (very strong) and 622 nm (weak, $^5D_0 \rightarrow {}^7F_2$), 652 nm (very weak, $^5D_0 \rightarrow {}^7F_3$), and 690 and 703 nm (weak, $^5D_0 \rightarrow {}^7F_4$).[17] It is well-known that the $^5D_0 \rightarrow {}^7F_2$ transition of Eu(III) ion is electric–dipole and extremely sensitive to chemical bonds in the vicinity of the Eu(III) ion. It is documented that the emission intensity increases as the site symmetry of Eu(III) ion decreases, suggesting the strong symmetry dependence of the $^5D_0 \rightarrow {}^7F_2$ transition.[17b,18] In contrast, the $^5D_0 \rightarrow {}^7F_1$ transition whose emission intensity is mainly dependent on the crystal field around the Eu(III) ion is magnetic–dipole and insensitive to site symmetry. The Eu ($^5D_0$) lifetime ($\lambda_{ex,em}$ = 397, 614 nm) of **6** is measured to be 1.3 ms. The emission spectrum of compound **8** at the excited wavelength 379 nm exhibits the characteristic emission of Tb^{3+} (see Fig. 5c).

These emission bands are 487 and 491 nm (weak, $^5D_4 \rightarrow {}^7F_6$), 544 (very strong) and 549 nm (weak, $^5D_4 \rightarrow {}^7F_5$), 584 and 589 nm (very weak, $^5D_4 \rightarrow {}^7F_4$), and 622 nm (very weak, $^5D_4 \rightarrow {}^7F_3$).[4a,11,19] Among these emission lines, the most striking green luminescence ($^5D_4 \rightarrow {}^7F_5$) for compound **8** is observed in the emission spectrum. The Tb ($^5D_4$) lifetime ($\lambda_{ex,em}$ = 379, 544 nm) of compound **8** is 1.8 ms. The splitting of transition bands in compounds **6** and **8** is due to crystal field splitting. Compound **9** is yellow-luminescent in the solid state when excited at 366 nm (see Fig. 5d). In the emission spectrum of compound **9**, two characteristic bands can be seen, which are attributed to transitions of 479 nm ($^4D_{9/2} \rightarrow {}^6H_{15/2}$) and 574 nm ($^4D_{9/2} \rightarrow {}^6H_{13/2}$).[16] To identify luminescent behaviors of dehydrated samples, compound **6** will be discussed in detail as a representation (see Fig. 5b). The luminescence spectrum recorded after the release of solvate water molecules is similar to that for compound **6** with solvate water molecules, however, the intensities of the emission bands for this dehydrated sample are significantly enhanced. The lower intensities of the emission bands for that hydrated compound are due to the quenching effect of the

luminescent state by high-frequency vibrating water molecules.[6a] Compared with the emission spectra of the four compounds (**5**, **6**, **8**, and **9**), the transition intensity of compound **5** is the weakest. The low emission intensity for Sm^{3+} ions imply that the efficiency of energy-transfer from organic ligands to metals is lower than that to Eu^{3+}, Tb^{3+} and Dy^{3+} in the lanthanide compounds.

Conclusions

Eleven new lanthanide oxalatophosphonate hybrids with a 2D layered structures, namely, $[Ln(H_3L)(C_2O_4)]\cdot 2H_2O$ (Ln = La–Dy, Er and Y, $H_4L = C_6H_5CH_2N(CH_2PO_3H_2)_2$), have been synthesized under hydrothermal conditions. Compounds **1–11** are isomorphous and they exhibit a 2D framework structure. Two $\{LnO_8\}$ polyhedra and four $\{CPO_3\}$ tetrahedra are interconnected into a unit *via* corner-sharing, and the so-built units are bridged by the oxalate anions into a layer. The result of connections in this manner is the formation of a 24-atom window. Thermal stabilities and guest desorption–sorption properties of compounds **1–11** have been investigated. Our studies show that the dehydrated solids of these compounds may be potential reversible adsorbent materials for water molecules. Luminescence properties of compounds **5**, **6**, **8** and **9** have also been studied. Compared with the emission spectra of the four compounds (**5**, **6**, **8**, and **9**), the transition intensity of compound **5** is the weakest. Compounds **6** and **8** showed red and green luminescence with a lifetime of 1.3 and 1.8 ms, respectively. Compared with the emission spectra of hydrated and dehydrated sample of compound **6**, the lower intensities of the emission bands for that hydrated compound are due to the quenching effect of the luminescent state by high-frequency vibrating water molecules. The results of our study indicate that by introduction of oxalate as the second ligand, we can obtain lanthanide oxalatophosphonates with good crystals and new structures as well as strong luminescence.

Acknowledgements

Notes and references

1 (a) J. D. Wang, A. Clearfield and G. Z. Peng, *Mater. Chem. Phys.*, 1993, **35**, 208; (b) G. Alberti and U. Costantino, in *Comprehensive Supramolecular Chemistry*, ed. J. M. Lehn, Pergamon-Elsevier Science Ltd, London, 1996, p. 1; (c) C. Y. Ortiz-Avila, C. Bhardwaj and A. Clearfield, *Inorg. Chem.*, 1994, **33**, 2499; (d) K. Maeda, Y. Kiyozumi and F. Mizukami, *J. Phys. Chem. B*, 1997, **101**, 4402; (e) F. Odobel, B. Bujoli and D. Massiot, *Chem. Mater.*, 2001, **13**, 163; (f) S. Cheng, G. Z. Peng and A. Clearfield, *Ind. Eng. Chem. Prod. Res. Dev.*, 1984, **23**, 2; (g) G. Cao, H. G. Hong and T. E. Mallouk, *Acc. Chem. Res.*, 1992, **25**, 420; (h) T. E. Mallouk and J. A. Gavin, *Acc. Chem. Res.*, 1998, **31**, 209; (i) A. Clearfield, *Chem. Mater.*, 1998, **10**, 2801; (j) T. Kimura, *Chem. Mater.*, 2003, **15**, 3742; (k) G. E. Fanucci, J. Krzystek, M. W. Meisel, L. C. Brunel and D. R. Talham, *J. Am. Chem. Soc.*, 1998, **120**, 5469.

2 (a) Z. Chen, Y. Zhou, L. Weng, C. Yuan and D. Zhao, *Chem.–Asian J.*, 2007, **2**, 1549; (b) J. Wu, H. Hou, H. Han and Y. Fan, *Inorg. Chem.*, 2007, **46**, 7960; (c) C. N. R. Rao, S. Natarajan and R. Vaidhyanathan, *Angew. Chem., Int. Ed.*, 2004, **43**, 1466; (d) P. J. Byrne, D. S. Wragg, J. E. Warren and R. E. Morris, *Dalton Trans.*, 2009, 795; (e) A. Clearfield, *Dalton Trans.*, 2008, 6089; (f) K. Maeda, *Microporous Mesoporous Mater.*, 2004, **73**, 47.

3 (a) Z.-H. Zhang, Y. Song, T. Okamura, Y. Hasegawa, W. Y. Sun and N. Ueyama, *Inorg. Chem.*, 2006, **45**, 2896; (b) X.-D. Zhu, J. Lu, X.-J. Li, S.-Y. Gao, G.-L. Li, F.-X. Xiao and R. Cao, *Cryst. Growth Des.*, 2008, **8**, 1897; (c) W.-S. Liu, T.-Q. Jiao, Y.-Z. Li, Q.-Z. Liu, M.-Y. Tan, H. Wang and L.-F. Wang, *J. Am. Chem. Soc.*, 2004, **126**, 2280; (d) O. Sato, T. Iyoda, A. Fujishima and K. Hashimoto, *Science*, 1996, **271**, 49; (e) T. M. Reinke, M. Eddaoudi, M. Fehr, D. Kelley and O. M. Yaghi, *J. Am. Chem. Soc.*, 1999, **121**, 1651.

4 (a) S.-S. Bao, L.-F. Ma, Y. Wang, L. Fang, C.-J. Zhu, Y.-Z. Li and L.-M. Zheng, *Chem.–Eur. J.*, 2007, **13**, 2333; (b) J. M. Lehn, *Angew. Chem., Int. Ed. Engl.*, 1990, **29**, 1304; (c) B. Zhao, X.-Y. Chen, P. Cheng, D.-Z. Liao, S.-P. Yan and Z.-H. Jiang, *J. Am. Chem. Soc.*, 2004, **126**, 15394; (d) Y. J. Kim, M. K. Suh and D. Y. Jung, *Inorg. Chem.*, 2004, **43**, 245.

5 (a) F. Serpaggi and G. Ferey, *Inorg. Chem.*, 1999, **38**, 4741; (b) F. Serpaggi and G. Ferey, *J. Mater. Chem.*, 1998, **8**, 2749; (c) A. Clearfield, C. V. K. Sharma and B.-L. Zhang, *Chem. Mater.*, 2001, **13**, 3099; (d) H. L. Ngo and W.-B. Lin, *J. Am. Chem. Soc.*, 2002, **124**, 14298; (e) O. R. Evans, H. L. Ngo and W.-B. Lin, *J. Am. Chem. Soc.*, 2001, **123**, 10395; (f) J. Plutnar, J. Rohovec, J. Kotek, Z. Zak and I. Lukes, *Inorg. Chim. Acta*, 2002, **335**, 27; (g) S. W. A. Bligh, N. Choi, C. F. G. C. Geraldes, S. Knoke, M. McPartlin, M. J. Sanganee and T. M. Woodroffe, *J. Chem. Soc., Dalton Trans.*, 1997, 4119.

6 (a) J.-L. Song, C. Lei and J.-G. Mao, *Inorg. Chem.*, 2004, **43**, 5630; (b) J.-L. Song and J.-G. Mao, *Chem.–Eur. J.*, 2005, **11**, 1417; (c) S.-M. Ying and J.-G. Mao, *Cryst. Growth Des.*, 2006, **6**, 964.

7 (a) Y.-Y. Zhu, Z.-G. Sun, H. Chen, J. Zhang, Y. Zhao, N. Zhang, L. Liu, X. Lu, W.-N. Wang and F. Tong, *Cryst. Growth Des.*, 2009, **9**, 3288; (b) L. Liu, Z.-G. Sun, N. Zhang, Y.-Y. Zhu, X. Lu, F. Tong, W.-N. Wang and C.-Y. Huang, *Cryst. Growth Des.*, 2010, **10**, 406; (c) Y.-Y. Zhu, Z.-G. Sun, Y. Zhao, J. Zhang, X. Lu, N. Zhang, L. Liu and F. Tong, *New J. Chem.*, 2009, **33**, 119; (d) N. Zhang, Z.-G. Sun, Y.-Y. Zhu, J. Zhang, L. Liu, C.-Y. Huang, X. Lu, W.-N. Wang and F. Tong, *New J. Chem.*, 2010, **34**, 2429; (e) Y. Zhao, J. Li, Z.-G. Sun, J. Zhang, Y.-Y. Zhu, X. Lu, L Liu and N. Zhang, *Inorg. Chem. Commun.*, 2008, **11**, 1057.

8 K. Moedritzer and R. R. Irani, *J. Org. Chem.*, 1966, **31**, 1603.

9 G. M. Sheldrick, *SHELXS-97, Program for solution of crystal structures*, University of Göttingen, Germany, 1997.

10 M. G. B. Drew, *Coord. Chem. Rev.*, 1977, **24**, 179.

11 Y.-Q. Guo, S.-F. Tang, B.-P. Yang and J.-G. Mao, *J. Solid State Chem.*, 2008, **181**, 2713.

12 K. Nakamoto, *Infrared and Raman Spectra of Inorganic and Coordination Compounds, Part A: Theory and Applications in Inorganic Chemistry*, Wiley, New York, 1997.

13 (a) A. Cabeza, M. A. G. Aranda and S. Bruque, *J. Mater. Chem.*, 1999, **9**, 571; (b) H. S. Martínez-Tapia, A. Cabeza, S. Bruque, P. Pertierra, S. García-Granda and M. A. G. Aranda, *J. Solid State Chem.*, 2000, **151**, 122.

14 A. Cabeza, M. A. G. Aranda and S. Bruque, *J. Mater. Chem.*, 1998, **8**, 2479.

15 (a) A. Cabeza, X. Ouyang, C. V. K. Sharma, M. A. G. Aranda, S. Bruque and A. Clearfield, *Inorg. Chem.*, 2002, **41**, 2325; (b) Z.-M. Sun, J.-G. Mao, B.-P. Yang and S.-M. Ying, *Solid State Sci.*, 2004, **6**, 295.

16 J. Xia, B. Zhao, H.-S. Wang, W. Shi, Y. Ma, H.-B. Song, P. Cheng, D.-Z. Liao and S.-P. Yan, *Inorg. Chem.*, 2007, **46**, 3450.

17 (a) J.-G. Mao, *Coord. Chem. Rev.*, 2007, **251**, 1493; (b) X.-F. Li, T.-F. Liu, Q.-P. Lin and R. Cao, *Cryst. Growth Des.*, 2010, **10**, 608.

18 (a) A. de Bettencourt-Dias, *Inorg. Chem.*, 2005, **44**, 2734; (b) G. L. Law, K. L. Wong, X. Zhou, W. T. Wong and P. A. Tanner, *Inorg. Chem.*, 2005, **44**, 4142.

19 S. F. Tang, J.-L. Song, X.-L. Li and J.-G. Mao, *Cryst. Growth Des.*, 2006, **6**, 2322.